

# Effects of Mn on fracture behaviour of DO<sub>3</sub> Fe<sub>3</sub>Al-based intermetallic alloy

LOU BAIYANG

*Department of Mechanical Engineering, Zhejiang University of Technology, Hangzhou 310014, People's Republic of China*

X. B. ZHANG, LIU MAOSEN

*Department of Materials Science and Engineering, Zhejiang University, Hangzhou 310027, People's Republic of China*

Z. ZHANG

*Beijing Laboratory of Electron Microscopy, Chinese Academy of Science, P.O. Box 2724, Beijing 100080, People's Republic of China*

The fracture behaviour of DO<sub>3</sub> Fe<sub>3</sub>Al-based intermetallic alloys with and without Mn (1.5 at %) were investigated by tensile tests (TT), transmission electron microscope (TEM) and scanning electron microscope (SEM). The results show that the addition of Mn could improve mechanical properties of the alloy, including room temperature ductility and high temperature strength. DO<sub>3</sub> Fe–28Al fractured in a transgranular cleavage mode at room temperature and it gradually changed to a ductile style with temperature increasing, whereas the sample with addition of Mn fractured mainly in a mixed intergranular–transgranular cleavage mode. Three major factors are considered to have effect of Mn on fracture behaviour of the alloys: reducing grain size, promoting slip and cross slip and enhancing cleavage strength. © 1998 Chapman & Hall

## 1. Introduction

Brittle fracture is always an engineering problem. Fe<sub>3</sub>Al-based intermetallic alloys characteristically exhibit limited ductility which is an obstacle to their applications, though they have many excellent properties such as good oxidation resistance, low density and certain high temperature strength. Theoretically, Fe<sub>3</sub>Al-based intermetallic alloys were thought to be essentially plastic at ambient temperature because they have more than five independent slip systems along {110} <111> in polycrystalline deformation and should have adequate ductility. Previous investigations have mainly attributed brittle behaviour of the alloys to environmental embrittlement, atomic bonds, bond polarization and ordering [1–6], and great efforts have been made to produce the alloys with both better room temperature ductility and high temperature strength; however, the achievements were very limited. Among them the addition of some alloying elements such as Cr, Ti, Mg, B, Ce in the alloys were reported to improve the mechanical properties of Fe<sub>3</sub>Al and FeAl alloys [7–10]. One notable result showed by McKamey *et al.* that the addition of alloying element Cr increases the ductility of the alloys significantly [11], but decreases the yield strength at room temperature.

Recently, some attentions have been paid to the addition of manganese in Fe<sub>3</sub>Al alloys. Yan *et al.* [11] reported their compressive tests for Fe–25Al and

Fe–25Al–4Mn at room temperature, showing that pure Fe<sub>3</sub>Al starts to crack at a strain about 10%, whereas the alloy containing Mn did not crack until a compressive strain of 30%. Li *et al.* [12] compared Fe–36.5Al with Fe–36.5Al–2Mn and found that Mn addition increases both the ductility and strength of B<sub>2</sub> Fe–36.5%Al alloy at room temperature. However, the evidence seems still not enough for showing the effect of Mn addition on the tensile properties of the alloys and little knowledge is known about the alloying mechanism.

Our preliminary studies have shown that Mn is an effective element for improving room temperature ductility and strength [13, 14]. The present paper tries to study tensile fracture behaviour of DO<sub>3</sub> Fe<sub>3</sub>Al-based alloys with and without Mn at different temperature.

## 2. Experimental procedure

Two DO<sub>3</sub>-ordered Fe<sub>3</sub>Al-based alloys Fe–28%Al and Fe–28%Al–1.5%Mn (atomic percent) were studied. The alloys were made in a vacuum induction furnace and cast into moulds. After homogenizing for 4 h at 950 °C, the alloys were hot-rolled at 950 °C and warm-rolled at 650 °C from 7 mm to 0.7 mm. Tensile samples were punched from the sheet and then heat treated in air for 1 h at 800 °C for recrystallization and for 50 h at 450 °C for DO<sub>3</sub> ordering. The tensile tests were performed at temperatures between 25 °C and 700 °C

in air with a strain rate of  $3.3 \sim 5 \times 10^{-2} \text{ s}^{-1}$  on an LX-250 kg tensile machine. The microstructures and fracture surfaces of above samples were examined by optical microscope and DXS-X2 electron microscope at room temperature; elemental line scanning and mapping was performed by electron probe X-ray analyser. Discs of 3 mm diameter were prepared for transmission electron microscopy (TEM) observation first by mechanical polishing and then by electropolishing in a nitric acid and methanol (1:4) electrolyte using Struers Tenupol-2 jet polishing unit at  $-28^\circ\text{C}$ . The Jeol JEM 100CX and Philips CM12 electron microscopes operated at 120 kV with double tilt stage were used for this study. Computer simulation based on electronic theory was performed to analyse the possible change of electronic valency and bond energy after Mn addition.

### 3. Results and discussion

#### 3.1. Mechanical properties

The tensile tests were performed over the temperature range of  $25\text{--}700^\circ\text{C}$  for the base alloy and the alloy containing 1.5% Mn (Fig. 1). Fig. 1 shows that both 0.2% yield strength and ultimate strength at room temperature were increased to 384.1 MPa and 487.0 MPa, respectively, for the alloy with Mn compared to 375.3 MPa and 441.2 MPa for the base alloy (Fig. 1a and b). With the temperature increasing, the 0.2% yield strength and the ultimate strength of Mn-containing samples became even much higher than that of base alloys, they reached the highest values at  $500^\circ\text{C}$  (yield strength was 70% higher than that of the alloy without Mn). It is interesting to notice that the strength of Mn containing samples still remained high (comparable to the highest value at  $500^\circ\text{C}$ ) at temperatures higher than  $500^\circ\text{C}$ , while the strengths of the base alloy already dropped dramatically. Another significant change with Mn addition was room temperature elongation which increased from 2% for the base alloy to 3.5% for the alloy with Mn addition (Fig. 1c). The elongation of both alloys increased with increasing temperature and rapidly increased as temperature higher than  $500^\circ\text{C}$  for the base alloy and  $600^\circ\text{C}$  for the alloy with Mn.

#### 3.2. Microstructures

The structures of base alloy and the alloy with Mn were observed by optical microscopy. The observed results are shown that the average grain size was much smaller in the alloy with 1.5%Mn addition (about  $50 \mu\text{m}$ ) than that in the base alloy (about  $95 \mu\text{m}$ ) and there was no general precipitation in the grains or grain boundaries in all of the samples added with Mn, indicating that the solubility limit for manganese in Fe-28Al alloy has not been reached. The face scanning of  $\text{MnK}_\alpha$  of the above specimen in Fig. 2 shows that the distribution of manganese is uniform in the alloy and no significant enriching of manganese was found at grain boundaries.

The  $\text{DO}_3$   $\text{Fe}_3\text{Al}$ -based alloys exist typically as two types of antiphase domains (APD): thermal APD and

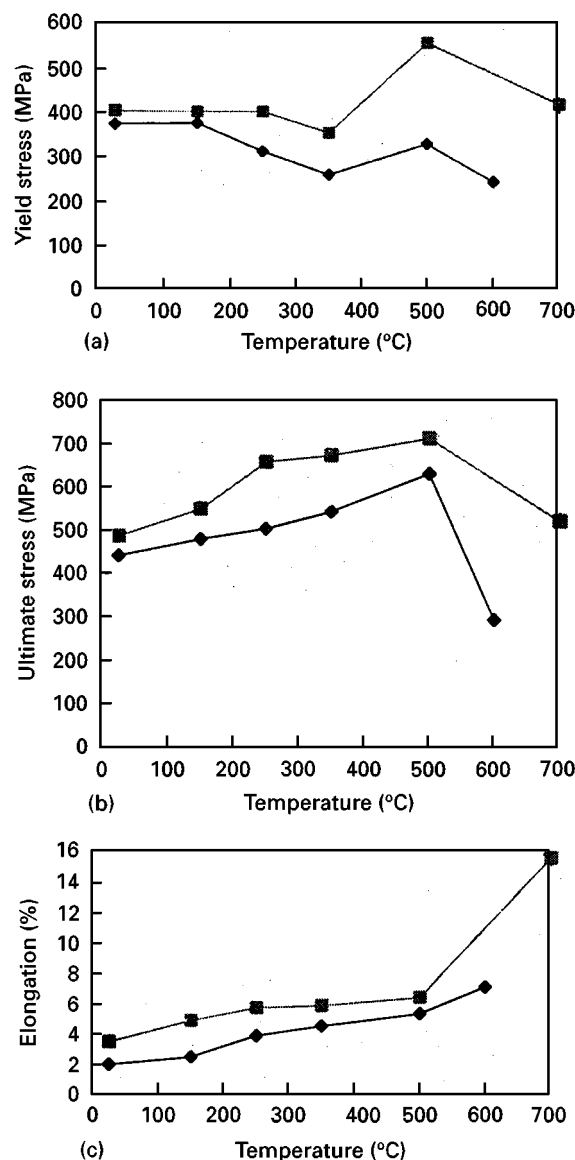


Figure 1 Tensile properties of  $\text{DO}_3$  Fe-28Al (◆) and Fe-28Al-1.5Mn (■) alloys.

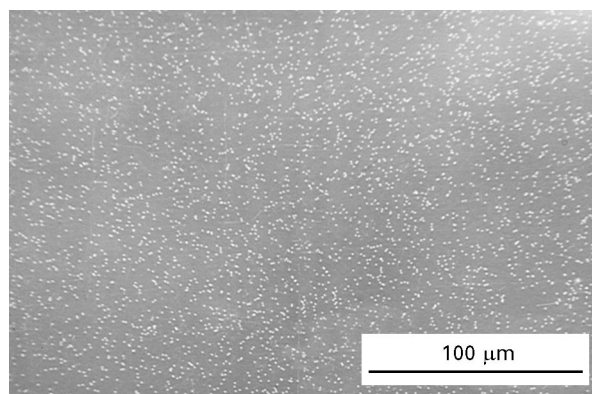


Figure 2 Electron probe micrographs of manganese in Fe-28Al-1.5Mn.

deformed APD. Electron diffraction pattern with  $[\bar{1}10]$  axis of Fe-28%Al-1.5%Mn specimen shows  $\langle 111 \rangle$  superlattice reflections of  $\text{DO}_3$  type (Fig. 3a), suggesting that manganese addition does not change the type of ordered phase of the alloy. Dark field

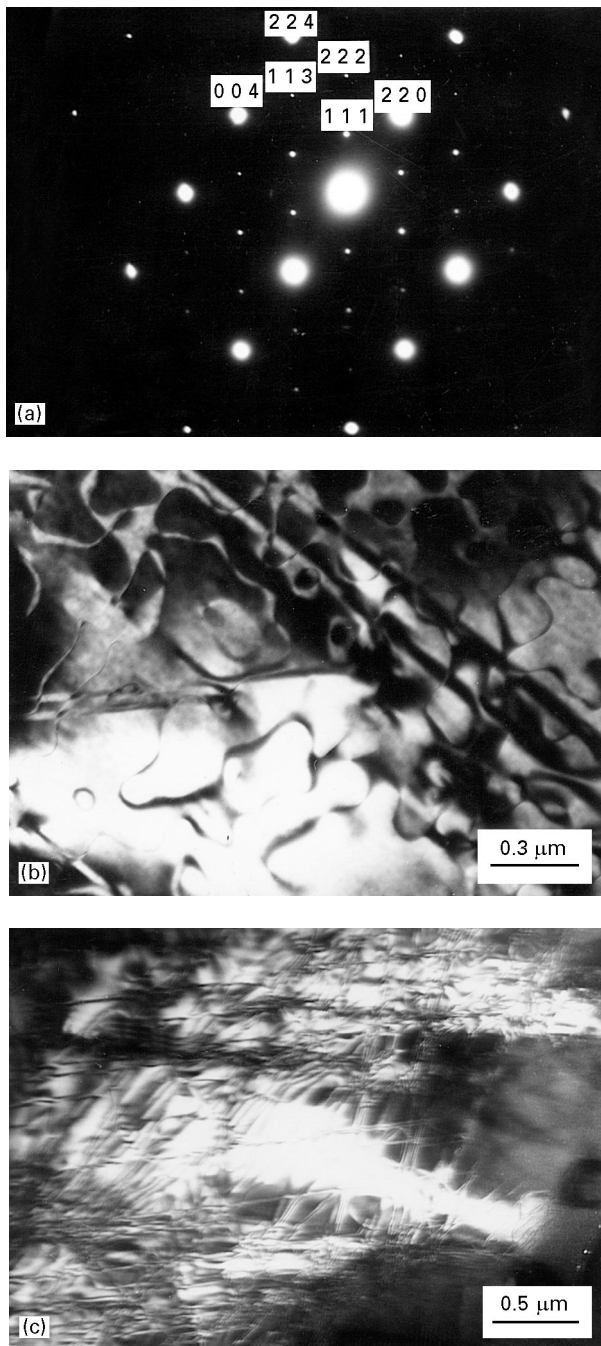


Figure 3 Electron diffraction pattern at  $[\bar{1}10]$  (a) and TEM micrographs of antiphase domains of Fe–28%Al–1.5Mn after small (b) deformation and (c) fracture.

electron micrograph using above reflection clearly shows two kinds of antiphase domain boundaries (APBs) in the alloys with Mn corresponding to the states before and after deformation respectively (Fig. 3b and c). An average diameter of 150 ~ 250 nm for the thermal domains was observed in the alloy with Mn (Fig. 3b), which is also smaller than the value of 250 ~ 350 nm reported for the alloys without Mn [15, 16]. The reduction of grain and APD size in our alloys with Mn addition could be an important factor responding to the improvements of ductility, specially of the strength both at ambient and elevated temperatures.

The relationship between grain size and yield strength is established from dislocation pile-up

mechanisms by Equation 1 [17–19]

$$\sigma_y = \sigma_0 + k(d^{-1/2}) \quad (1)$$

where  $\sigma_y$  is the yield strength,  $\sigma_0$  is a reference stress,  $k$  is a material constant, and  $d$  is the grain size. This equation indicates that as the grain sizes decrease, the yield strength increases. Reduction of grain size decreases dislocation block and retards formation of cleavage crack at grain boundaries which is beneficial to increase both the ductility and strength even at elevated temperatures. In addition to the change of grain size, the APD size for the alloy added with manganese is also reduced from an average of 330 nm [15, 20] to 150 ~ 250 nm; the same phenomenon was also reported by Athanassiadis *et al.* [16] where APD size was gradually reduced from 500 to 100 nm after the Mn addition up to 10 at %. Smaller APD creates more domain boundaries and would, of course, produce better mechanical properties of the alloy. Other ternary additions studied previously with no change of the grain and APD size also resulted in a shift to intergranular failure but often with a reduction in yield strength [1], which implied the reduction of grain size with Mn addition did indeed play an important role specially in raising the strength of the alloys.

After deformation the morphology of APBs were completely changed from random curves into crossed lines. Fig. 3(c) shows the deformed APBs in a fractured specimen, whose higher density of deformed zigzag APBs suggest that cross-slips of superlattice dislocations took place frequently when the alloy deformed.

To examine the influence of Mn addition on the slip behaviour, slightly deformed samples (1.5%) were prepared under tension at room temperature and slip lines on the surface of both alloys observed by optical microscope are shown in Fig. 4a. Straight slip lines which are parallel to each other and aligned in the same direction within individual grains on the surface of the base alloy, suggesting no cross slipping happened and only one slip system was generated in this alloy. In contrast, slip lines in the alloy with Mn addition become finer, denser and wavy (Fig. 4b); some slip lines even passed through grain boundaries, indicating that not only slipping was easier to take place but cross slip was also generated during the deformation in the alloy after Mn addition. Therefore, Mn addition could promote more cross slip processes to occur when the alloy was deformed and then increase ductility of the alloy.

### 3.3. Tensile fracture

Fig. 5 shows different morphologies of fracture surfaces cracked at room temperature of the above two alloys. Fe–28Al alloy without Mn cracked in a cleavage mode (Fig. 5a). Its cleavage planes are much larger than that of Mn-added samples (Fig. 5b) and many parallel secondary cracks exist, indicating that the cracks can propagate easier inside the grains and the base alloy is obviously brittle. On the other hand, cleavage and intergranular mixed fracture and many

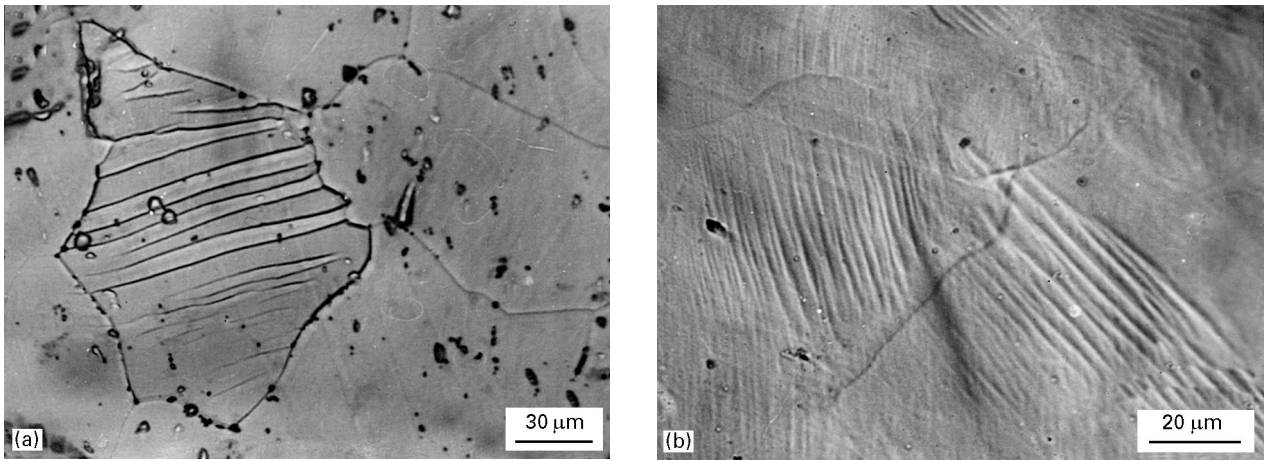


Figure 4 Slip lines produced in tension at room temperature showing (a) coarse, straight slip in Fe-28%Al and (b) wavy and finer slip in Fe-28%Al-1.5%Mn.

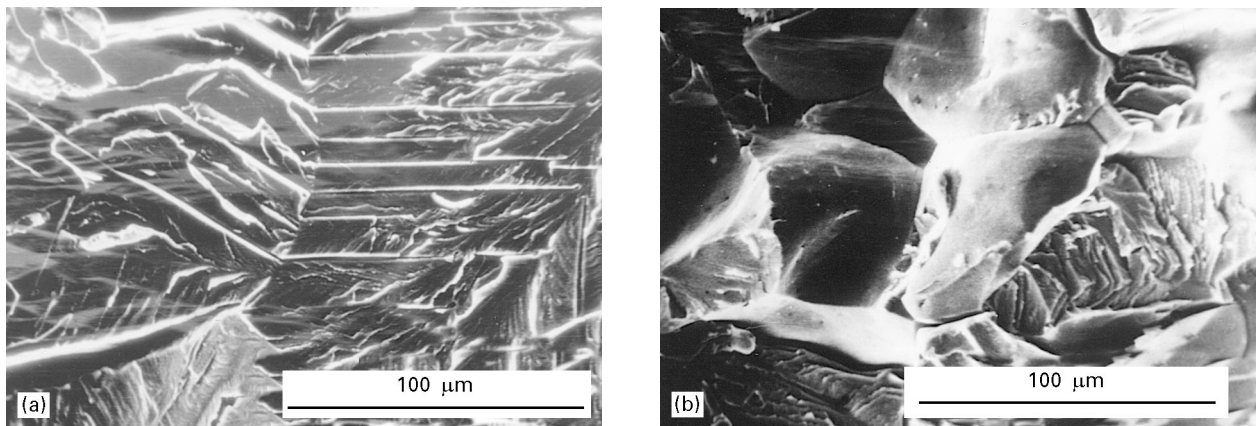


Figure 5 Fracture surface produced in tensile at room temperature, showing (a) a transgranular cleavage fracture mode in Fe-28%Al and (b) a mixed transgranular cleavage-intergranular fracture mode in Fe-28%Al-1.5%Mn.

small rippled cleavage steps were observed for the  $DO_3$  alloy with Mn addition (Fig. 5b), which indicates that the addition of Mn increases the ductility of the alloy and changes the fracture mode from transgranular cleavage to mixed intergranular-transgranular cleavage at room temperature. It was also observed from Fig. 5 that the grain size is much smaller in the alloy with Mn than in the alloy without Mn.

The morphologies of fracture of the alloy without Mn at temperatures from 150 to 350 °C are mainly cleavable (Fig. 6a-c), which shows fewer secondary cracks in comparison to ambient temperature fracture and river pattern formed by a major cleavage crack propagating together with some small ripped cleavage steps. The cleavage planes became small and some small cavities appeared in the 250 °C fracture. As testing temperature reached to 350 °C, more cavities were observed, not only in boundaries but also inside the grains (Fig. 6c). Significant change of the fracture pattern occurred at 500 °C, at that temperature a complete cavitation mode was formed (Fig. 6d), indicating that the ductility of the alloy increases with the increasing temperature.

For  $DO_3$  Fe-28Al-1.5Mn alloy, the fracture mode also changed gradually from brittle fashion to ductile at elevated temperatures (Fig. 7), but in different ways

and by different processes in contrast to the alloy without Mn. The cleavage and intergranular mixed fracture still is the main failure feature at 250 °C, which is rather similar to the case of the same sample fractured at ambient temperature, only the secondary cracks decreased. Small cavities occur on most fracture planes when the alloy was tested at 500 °C and the fracture mode is evidently changed to an intergranular-cavitation mixed fashion. As temperature reached to 700 °C, the alloy fractured completely in a ductile way of cavitation fashion, no intergranular or cleavage failures could be observed.

The electronic valency and bond energy were calculated according to electronic theory to analyze the possible change of atomic bond strength after Mn addition. Table I shows the main results of the above analysis [15], which indicates: (a) the bond strengths in  $\langle 100 \rangle$  direction for both alloys were weaker than that in  $\langle 111 \rangle$  direction, it means the cleavage would take place in  $\{100\}$  planes instead of  $\{111\}$  for both alloys; (b)  $\langle 100 \rangle$  bond strength is 23% increased after Mn addition.

The base alloys usually fracture in form of cleavage failure and (or) intergranular failure at room temperature, in which way the alloys fracture is of course dependent on their relative strength to each other.

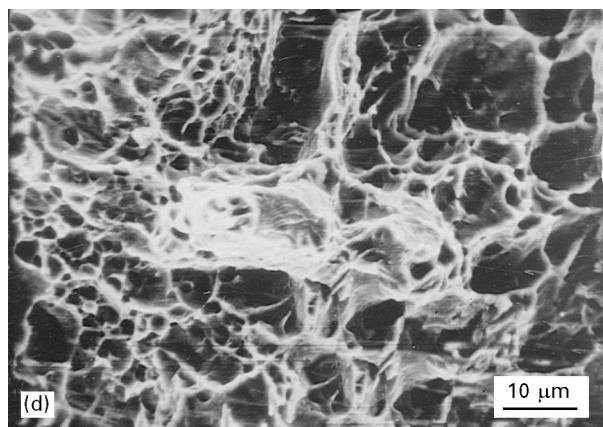
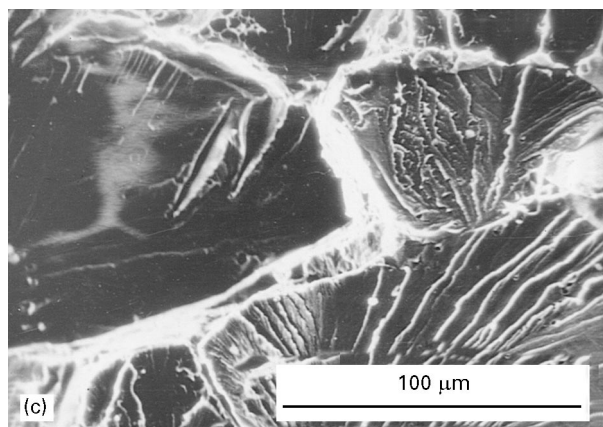
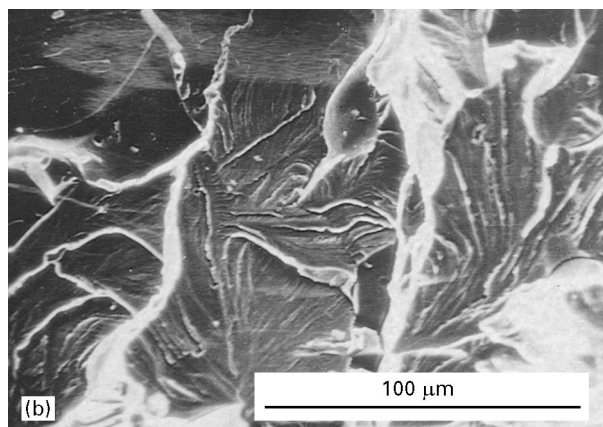
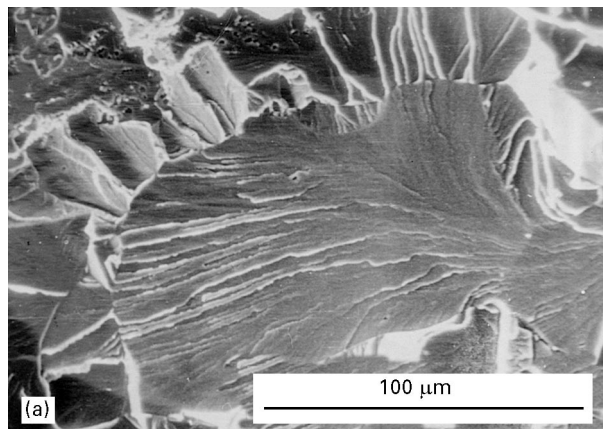


Figure 6 Fracture surfaces of Fe-28Al alloy tensing at elevated temperatures (a) 150 °C, (b) 250 °C, (c) 350 °C and (d) 500 °C.

After Mn addition, the fracture mode shifts from transgranular cleavage to mixed intergranular-transgranular cleavage accompanying an increase of the yield and ultimate strength which indicates that the

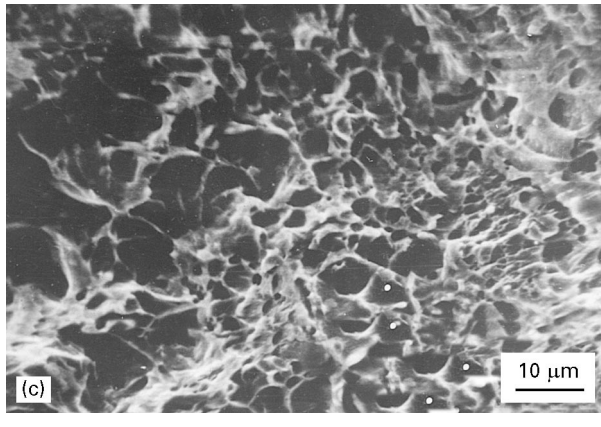
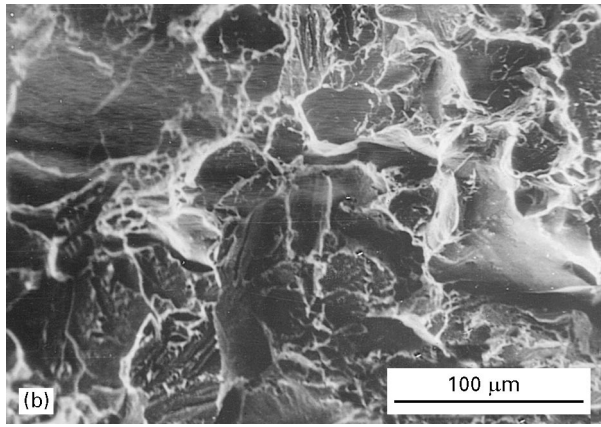
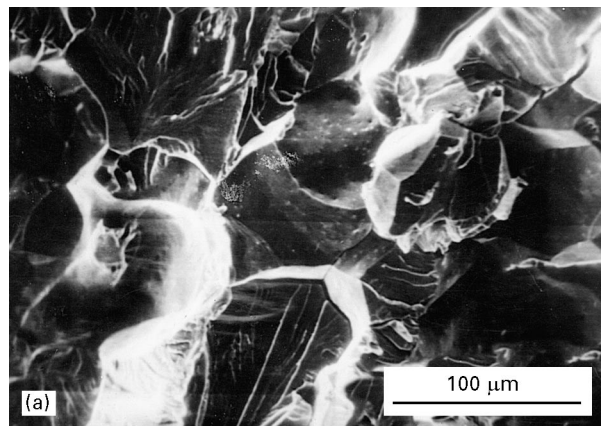


Figure 7 Fracture surfaces of Fe-28Al-1.5Mn alloy tensing at elevated temperatures (a) 250 °C, (b) 500 °C and (c) 700 °C.

cleavage strength is enhanced to a level comparable to intergranular strength after Mn addition because both cleavage and intergranular strengths are increased in accordance with the strength increasing. This situation is quite similar to that of the alloys added with Cr shown by McKamey *et al.* [1], only the yield strength was decreased in their case, showing that manganese is more sensitive to enhance strength of the alloy. Although it is still not very clear why alloying elements such as Mn and Cr could enhance the transgranular cleavage strength of the alloy, computer simulation of the bonding energy for the alloys with and without Mn, based on electronic theory [21], may give a reasonable explanation. It is shown in Table I that after addition of Mn, both  $\langle 100 \rangle$  and  $\langle 111 \rangle$  bonding strengths are evidently increased, while the cleavage planes remain along  $\{100\}$ , as is the case without Mn and it has been experimentally proved by

TABLE I Values of bond energy in DO<sub>3</sub>-ordered structure with and without Mn (kJ mol<sup>-1</sup>)

	Direction	$E_{Al-Fe}$	$E_{Fe-Fe}$	$E_{Al-Al}$	$E_{Al-Mn}$	$E_{Mn-Mn}$	$E_{Mn-Fe}$	$E_{total}$
Fe-28Al	$\langle 111 \rangle$	67.9371	30.4686					98.4057
	$\langle 100 \rangle$	8.2124	7.499	13.949				29.6604
Fe-28Al-1.5Mn	$\langle 111 \rangle$	67.6006	29.988		39.8754		17.691	155.155
	$\langle 100 \rangle$	8.2187	7.4837	13.9671		0.0016	6.8294	36.4905

Sun *et al.* [22]. According to the computer calculation,  $\langle 100 \rangle$  bonding strength for the alloy with addition of Mn is increased by 23%. Obviously, the stronger the bonding the higher the cleavage strength and the higher the fracture strength, therefore the fracture mode would shift from transgranular cleavage to a mixture of transgranular cleavage and intergranular fashion, which is obviously in good agreement with our experimental results. This enhancement in strength also results in an increase in elongation before the onset of failure.

#### 4. Conclusions

The addition of 1.5% manganese into DO<sub>3</sub> Fe-28Al alloy increases both ductility and strengths of the alloys at temperatures between 25 and 700 °C, which is mainly attributed to the reduced grain size and APD size, more slip and cross-slip. The addition of manganese enhances cleavage strength and partially suppresses cleavage failure, producing a change in the fracture mode from transgranular cleavage to a mixed cleavage and intergranular fashion.

#### Acknowledgement

The authors would like to express their thanks to Professor Xiao Yanling in the Department of Engineering, Zhejiang University of Technology, for help with SEM studies.

#### References

1. C. G. McKAMEY, J. A. HORTON and C. T. LIU, *J. Mater. Res.* **4** (1989) 1156.
2. C. T. LIU and E. P. GEORGE, *Scripta Metall.* **24** (1990) 1583.

3. D. J. DUQUETTE, *Mater. Sci. Eng.* **198A** (1995) 205.
4. C. L. FU and M. H. YOO, *Acta Metall.* **40** (1992) 703.
5. S. P. CHEN, A. F. VOTER and D. T. SROLOVITZ, in High-Temperature Ordered Intermetallic Alloy II, MRS Symposium Proceedings **81** (1987) p. 45.
6. M. J. MARCINKOWSKI, M. E. TAYLOR and F. X. KAYSER, *J. Mater. Sci.* **10** (1975) 406.
7. D. J. GAYDOSH, S. L. DRAPER and M. V. NATAL, *Metall. Trans. A* **20** (1989) 1701.
8. YIN WEIMIN, GUO JIANTING and HU ZHUANGQI, *Acta Metall. Sinica* **29** (1993) 193A.
9. SUN YANGSHAN, GUO JUN, ZHANG LINING and ZHANG JINPING, *ibid.* **27** (1991) 255A.
10. I. BAKER, O. KLEIN, C. NELSON and E. P. GEORGE, *Scripta Metall.* **30** (1994) 863.
11. YAN WEN, YANG YONG and LIU JIANGNAN, in The First Pacific Rim International Conference on Advanced Materials and Processing (PRICM-1), edited by Changxu Shi, Hengde Li and Alexander Scott (MMMS) (1992) p. 785.
12. LI DINGQING, LIN DONGLIANG, SHAN AIDANG and LIU YI, *Scripta Metall.* **30** (1994) 655.
13. LOU BAIYANG, LIU MAOSEN, TU JIANGPING, MAO ZHIYUAN, XIAO YANLING and ZHONG YINHONG, *Funct. Mater.* **26** (supplement) (1996) 545.
14. LOU BAIYANG, LIU MAOSEN, TU JIANGPING, MAO ZHIYUAN, XIAO YANLING and ZHONG YINHONG, *Trans. Met. Heat Treatment* **17** (1996) 58.
15. LOU BAIYANG, PhD Thesis, Zhejiang University 1996.
16. G. ATHANASSIADIS, A. LE CAER, J. FOCT and L. RIMLINGR, *Phys. Stat. Solidi* **40(a)** (1977) 425.
17. E. O. HALL, *Proc. Phys. Soc.* **B64** (1951) 747.
18. N. J. PETCH, *J. Iron Steel Inst.* **174** (1953) 25.
19. A. H. COTTRELL, "The mechanical properties of matter" (Wiley, New York, 1964) p. 282.
20. D. G. MORRIS, M. M. DADRAS and M. A. MORRIS, *Acta Metall. Mater.* **41** (1993) 97.
21. YU RUIHUANG, *Chinese Sci. Bull.* **23** (1978) 271.
22. SUN YANGSHAN, GUO JUN, ZHANG LINING and ZHANG JINPING, *Acta Metall. Sinica* **27(4)** (1991) A255.

Received 1 May  
and accepted 24 September 1997